P2.4

AN EVALUATION OF LIGHTNING FLASH CHARACTERISTICS USING LDAR AND NLDN NETWORKS WITH WARM SEASON SOUTHEAST TEXAS THUNDERSTORMS

Joseph W. Jurecka, National Weather Service, Lubbock, TX
Dr. Richard E. Orville, Texas A&M University

A comparison of flash parameters from the National Lightning Detection Network (NLDN) is made with data obtained from the Houston Lightning Detection and Ranging II (LDAR) network. This work focuses on relating the peak current and number of strokes in a negative flash (multiplicity) of lightning with the spatial extent and mean altitude of three-dimensional lightning in 1407 flashes as mapped by the LDAR network. It is shown that increasing negative multiplicities over the range two through ten exhibit, on average, a higher flash extent with higher multiplicities. Single-stroke flashes have mean heights of nearly 2 km greater. Higher order multiplicities (2 to 10+) were correlated with mean source heights near 8 km. Increasing multiplicity tends to be associated with greater flash extents increasing more horizontally than vertically with a 50% to 70% increase in flash extent. No obvious relationship between peak current and flash extent was observed. Examining peak current and mean height shows that low current flashes (<10kA) exhibit higher mean heights. However, this may be due to intra-cloud only flashes being reported as cloud to ground events by the NLDN. Bipolar flashes do not show much variation with height and flash extent with the exception of negative-first bipolar flashes, which exhibited mean flash extents twice that of other types. Finally, the flash detection efficiency is shown to be 99.7% within 60 km of the network center.

1. INTRODUCTION

Since the late 1980s, a National Lightning Detection Network (NLDN) for detecting cloud-to-ground strokes has been in place (Cummins et al, 1998 and Orville, 2008). More recently, technology has allowed the use of Very High Frequency (VHF) radio frequency emissions to detect individual energy sources within the flash. One such network is deployed, in the Houston area and is run by the Department of Atmospheric Sciences at Texas A&M University. The Houston network is formally known as the Houston Lightning Detection and Ranging (LDAR) network. Vaisala, Inc manufactures the sensors and central server.

By mapping the three dimensional information provided by the VHF network and combining the information with cloud-to-ground data, insight into the volumetric characteristics of total lightning becomes possible.

Many studies have analyzed NLDN and LDAR (or LMA) data. Generally, these examine single flashes or a small collection of events. However, a study analyzing thousands of comparisons between NLDN and LDAR data is new. This work fills that gap and provides a comparison for observations using NLDN and the Houston LDAR network. Although the two networks capture uniquely different information, temporal and spatial synchronization facilitates comparison between the two networks. This combination allows the analysis of "total lightning" within the thunderstorm. Via total lightning, we gain insight into storm structure, microphysical processes, and electrical nature of thunderstorms.

While the LDAR and NLDN data can be analyzed on a per-flash basis, this work focuses not on individual characteristics but rather the trends found among hundreds of flashes. As the research on this topic was ongoing, it was very apparent that lightning metrics exhibit significant flash-to-flash variance within the same storm a few seconds apart. As the storm matured, overall, events appeared to expand in extent along with the total volume of the storm. It is also recognized that different storm types will provide different signatures. For example, a summer time, low-shear thunderstorm along the Gulf Coast has a smaller volume than does a springtime mesoscale convective system. Even within a system, such as an MCS, there are differing characteristics within parts of the storm (Carey et al., 2005). This study is comprised of generally weakly forced multicell thunderstorms. Aggregating data from many flashes reveal trends between the NLDN and LDAR networks. Some relationships yield a nearly linear relationship. Others offer more complex characteristics such as anomalies associated with single-stroke flashes. Bipolar flashes, containing both positive and negative strokes, also appear to deviate from the characteristics of uni-polar events.

Southeast Texas is a climatologically active thunderstorm region throughout the year, which provides excellent opportunities for data gathering and analysis. Synoptic features, such as frontal convection as well as mesoscale influences such as the sea breeze, affect this region. The period of this study analyzes convection on selected days from May to July 2007. This time period, while providing near climatological averages of measurable rainfall, produced a higher than normal number of days with rainfall and therefore higher than average thunderstorm events. However, the individual thunderstorms themselves were typical of the season.

This analysis is best handled with discrete flashes that are often challenging to find in the cluster events of the season. However, with careful selection, it is possible to obtain isolated flash events within an otherwise chaotic lightning environment.

It seems logical that parameters collected by the NLDN, namely multiplicity and peak current, would be closely related to those determined by the LDAR network. There are a number of hypotheses that were tested with this work. Logic suggests that increasing peak current might require the support of increased flash extent. Likewise, an increase in multiplicity would also require the expanded flash extent. As charge regions have a finite charge capability, obtaining a larger volumetric charge region should enable the increased charge flow. Visual observation of spider lightning indicates that a large visible discharge occurs within the anvil region of mature thunderstorms spreading in a mostly horizontal extent. As a result, the flash extent is not expected to cubically grow with increasing flash extent but rather spread more horizontally. With these ideas in place, if multiplicity were increased, mean height should increase since the LDAR detects the presence of most sources at the 10 km level. If flash extent increases, especially horizontally in a narrow vertical band such as an anvil, the mean height should increase. Likewise, one would expect an increase of mean height to increase with peak current as well.

With regard to differing flash types, one might expect negative flashes, with higher average multiplicity, to exhibit higher flash extents and mean altitudes than positive flashes. Taking this idea one more step, bipolar events, which contain both positive and negative strokes, would be expected to exhibit characteristics similar to negative flashes.

2. THE HISTORY OF THREE DIMENSIONAL LIGHTNING DETECTION BY RADIO FREQUENCY METHODS

In 1967, F. J. Hewett suggested that a hyperbolic array of radio receivers might yield the ability to track storms. From this suggestion, intracloud lightning positioning studies using radio frequency (RF) methods began with an analog network located in South Africa in the late 1960s. This five station network, operated by the South African National Institute for Telecommunications Research, was used by D.E. Proctor to create the first representations of intracloud flash extent by observing the demodulated signal output of five 250 MHz receivers spaced in nearly a perpendicular array. End to end, this network stretched for approximately 40 km in a north-south and 30 km east-west configuration. Receiver outputs were connected to a central observing station where time-relative measurements of each atmospheric burst were displayed on cathode ray tubes and captured on 35mm film as seen in figure 2.1 (Proctor 1971).

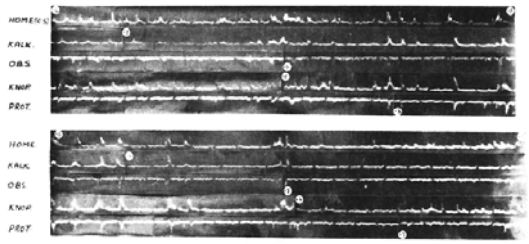

Figure 2.1 Received signals from single flash. Propagation delays from each of the five receiving sites has been removed [Source: Proctor 1971.]

The system was calibrated to eliminate internal propagation delays from the individual receivers to the observation point (Proctor 1971). After reception and film development, Proctor began the time-intensive task of manually associating each station's data with individual VHF sources based on the arrival time at each of the five sensors. By combining the data from the sensors, individual VHF source locations were derived and thus, the first three-dimensional mapping of intracloud lightning based on RF methods were produced as illustrated in figures 2.2 and 2.3. Both charts depict flashes occurring on March 26, 1970. While Proctor's work was time-intensive, his findings are remarkably similar to what is observed with today's lightning mapping networks. Horizontal accuracy was estimated to be on the order of 20m with a substantially larger (100m to 1km) vertical error.

In addition to the main channel discharges, he was able to capture stepped-leader and dart leader features. While not directly related to this work, it would be interesting to compare the findings of Proctor dealing with step and dart leaders with the visual observations made possible by high speed camera lightning research by Tim Samaras (2008).

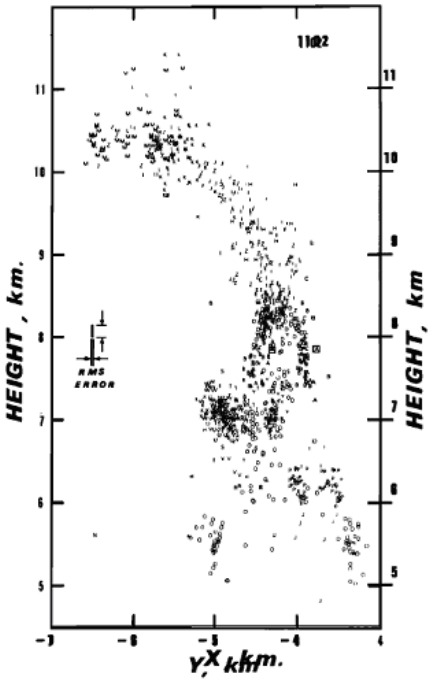

Figure 2.2 Derived projection of point sources shown for a single flash. The source of the first pulse to be received has been enclosed by a square [Source: Proctor 1981.]

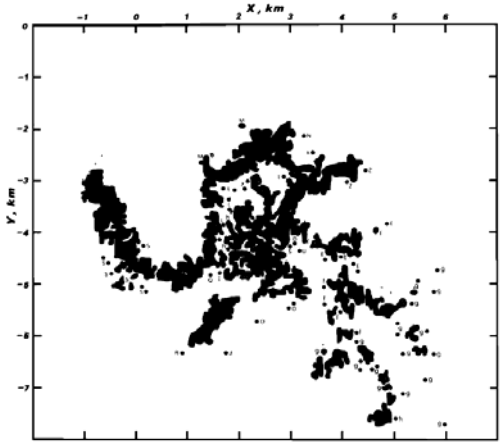

Figure 2.3 Plan view of flash obtained by locating 2640 point sources. In this map, isolated sources are shown as dots. The alphabetical symbols do not themselves represent the positions of sources [Source: Proctor 1981.]

Yet another critical piece of information, related to RF based lightning networks was determined by Proctor (1981). By comparing the incoming waveforms of demodulated output at 2, 30, 250, 600, and 1430 MHz, he concluded that lightning generates wideband signals on the order of many GHz. Lightning radiation is therefore not oscillatory in nature, but results in a broadband pulse-like waveform. This finding showed that the exact frequency of operation was indeed not critical and thus gave researchers confidence to proceed with studying a number of different frequency bands. Proctor had taken great care to design the radio system, with a sensitivity of 0.5 μV/m for 10 dB signal to noise ratio, for adequate spurious and intermediate frequency (IF) rejection. The radio system IF frequency was 30 MHz and Proctor understood that lightning RF bursts were 20dB stronger at 30 MHz than at the primary reception frequency of near 250 MHz. This occurs because it takes more energy to generate radio waves at higher frequencies. Thus, given equal energy, higher frequency emissions are lower in amplitude.

Proctor also took into consideration that the "backhaul" network, which relayed the signal data from each site to the observation station, could be susceptible to impulse noise as well thus potentially contaminating the VHF signal. In the absence of present data technology, X-band (near 10 GHz) telemetry links using Frequency Modulation (FM) were used. Lightning induced RF signatures are 26 dB weaker at 10 GHz than the primary reception frequency (Proctor 1971). Furthermore, the use of FM further desensitizes the link from static crashes within the demodulation limiter in much the same fashion that FM broadcasts are far less susceptible to noise than AM broadcasts on an ordinary radio. Other means of avoiding contamination were also used, further emphasizing the need for careful engineering practices when designing a lightning detection network.

In the mid 1970s, C.L Lennon and team at the Kennedy Space Center (KSC), Florida created a seven sensor network near the KSC. This network, named the Lightning Detection and Ranging (LDAR) network, is the predecessor of the system used in Houston today. The network operated between 30 and 50 MHz with sensors located in two Y shaped networks with a diameter of 20km and a common central station. Logarithmic receivers provided digitized signal information over a 100-microsecond interval with

a resolution of 50 nanoseconds (Krehbiel 1981). This network was capable of resolving several tens of events per flash and one such example appears in figure 2.4.

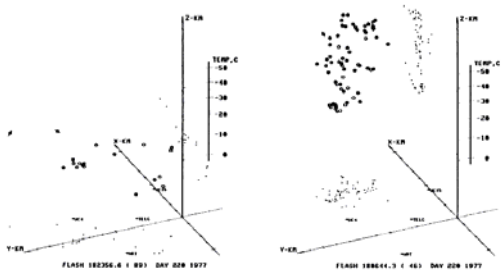

Figure 2.4 Example flashes from the early Kennedy Space Center Network. The X-Y axes illustrate the plan-view perspective with vertical extent displayed along the Z axis [Source: Krehbiel 1981.]

Further Refinements in RF based intracloud lightning continued and in the early 1990s, a second generation, seven site, LDAR system was developed at the Kennedy Space Center, which featured improved temporal resolution and number of events per second which theoretically allows the locating of several thousand sources per second (Maier et al. 1995 and Mazur et al. 1997). The improvement in mapping ability is depicted in figure 2.5. This technology was subsequently licensed to Vaisala for commercial deployment and, with additional minor enhancements such as remote frequency control, is the basis for the Houston LDAR II Network. The Dallas / Fort Worth network uses the same equipment as the Houston network, but currently has nine sensors. The reader is directed to Ely et al. (2008) for additional details about the Houston network during its operation at 69 MHz. A discussion of the Dallas Network is found in Carey et al. (2005).

In the late 1990s, a ten-site Lightning Mapping Array (LMA) was developed and deployed in the desert of New Mexico by the New Mexico Institute of Mining and Technology. This system uses a 6 MHz-bandwidth receiver tuned to the Television Channel 3 spectrum near 63 MHz and is capable of capturing 50 ns time resolution data that is phase locked to a GPS (Rison et al. 1999). The LMA design has been used in many locations including the National Severe Storms Forecast Laboratory (Mach et al. 1986), University of Alabama at Huntsville (Goodman et al. 2005), in the Washington D.C. area (Krehbiel et al. 2006), as well as during the STEPS project in Colorado and Kansas (Wiens et al. 2005).

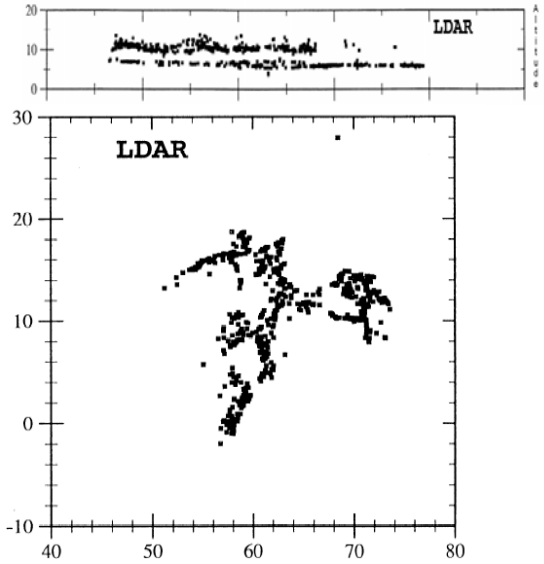

Figure 2.5 Example of LDAR detected flash. The top portion depicts activity in the vertical. Plan view depiction is located in the bottom portion. Plan view axes indicate the distance, in km, from the center of the network [Source: Mazur et al., 1997.]

The sensitivity of the LMA system is significantly better than that of the LDAR II network in Houston. The LDAR system is intended as an operational network and not optimized to extract as much data as possible (MacGorman and Rust 1998). One of the primary external impediments for the Houston network is RF contamination from a wide variety of sources. Whereas the LMA network in New Mexico detected pulses near -90 dBm, the Houston network minimum detectable signal level ranges from -60 dBm during particularly noisy periods at the worst sites to -80 dBm at the best. For this reason, aircraft and balloon trails, caused by collisions with ice particles, have never been observed on the Houston LDAR II network as they have with both the New Mexico Network and STEPS network (Thomas et al. 2004). An example of an aircraft trail is presented in figure 2.6.

Regardless of the decreased sensitivity, in comparing the appearance and extent of flashes in the published literature, the LMA system appears to have flash extents similar in appearance to those detected with the Houston network. Most notably, the LMA system displays lightning maps comprised of a much denser array of resolved points. As a result, it would appear that the decreased sensitivity of the

LDAR system in the Houston area, while affecting the density of plots, would not be expected to significantly change the resulting flash extents or altitudes. Arguably, with increased sensitivity, flash extents could increase somewhat, but the general trends found herein are expected to be similar to those found with an LMA network. That said, Mazur et. al. (1987) found that the detected three dimensional lightning data obtained using an interferometer showed a higher density of points at lower altitudes. Thus, is certainly appears that neither LDAR nor interferometric measurements individually capture all electromagnetic sources equally. As such, a bias is likely to exist when using LDAR data alone. In side by side comparisons, the LDAR data did appear to capture horizontal flash extent better than interferometers, but was poorer at more vertically oriented structures. It is believed, based on Mazur's findings that LDAR will likely capture horizontal flash extent more adequately, but a bias in the vertical may exist overall.

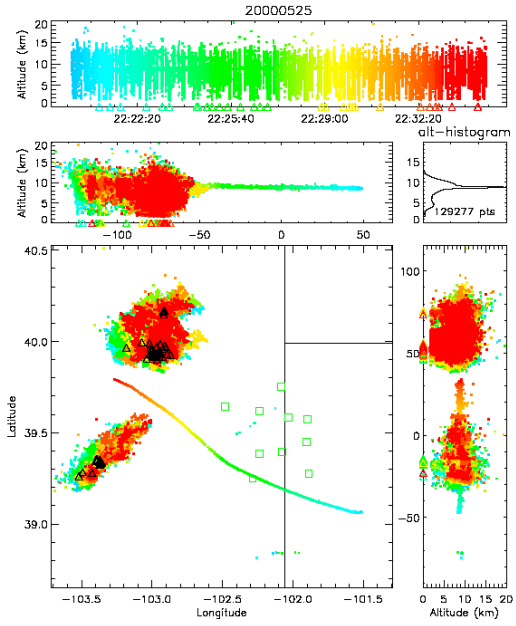

Figure 2.6 Aircraft track over Kansas and Colorado on 25 May 2000. The plane was flying from east to west at about 9 km altitude (29.5 left) and vectored between two electrically active storms. The airplane was tracked by the LMA because it was flying through an ice crystal cloud downwind of the storms that caused it to become charged and give off a steady stream of small sparks. The plane was tracked for 13 min over a 170 km distance and was presumably a commercial aircraft. Two other aircraft were more weakly detected over the center and to the south of the mapping network. The squares indicate the operational stations on this day; only sources located by seven or more stations are shown. The triangles indicate the location of negative polarity ground discharges. The distance scales are in latitude and longitude in the plan view and in kilometer units in the vertical projections [Source: Thomas et al. 2004.]

A number of studies have been conducted with the LMA/LDAR networks primarily to better understand the electrical nature of thunderstorms. In particular, several attempts to map the charge structure of storms have occurred including but not limited to the STEPS project in eastern Colorado and western Kansas in the summer of 2000 (e.g. Wiens et al. 2005).

Under the assumption that electrical breakdowns propagate into regions of opposing charge, it is possible to determine the charge polarity of different parts of the storm from the propagation of the flash in the cloud (e.g. Wiens et al. 2005). Figure 2.7 illustrates an LMA recorded flash after applying the polarity logic to a thunderstorm. With this effort, regions of positive and negative charge become clearly defined (Hamlin et al. 2003). Thunderstorms often display a tripole structure where there are two regions of positive charge (one near 0°C and one above -20°C) with a negative charge region sandwiched between these two at -10°C and -20°C. Some storms exhibit an inverted polarity structure as observed in Stolzenburg et al. (1998a) and Lang et al. (2004). Storms modify their structure, potentially becoming further stratified, during their lifetime with apparent dependencies on updraft strength (Wiens et al. 2005).

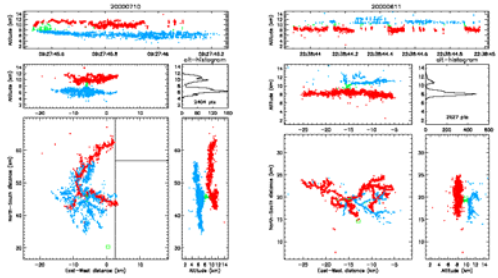

Figure 2.7 Example of two individual discharges detected by the LMA. The flash on the left is a classic, normal-polarity bi-level IC, while the right is an inverted polarity IC. The positive charge regions are colored by red/dark-gray points, and

the negative by blue/light-gray [Source: Hamlin et al. 2003.]

There are several articles in the literature that discuss charge polarity structures, flash rates, and flash patterns especially in individual storms. Wiens et al. (2005) examined several, mostly isolated, storms in Colorado and Kansas and hypothesized that the LMA system tends to more readily capture negative breakdown into positive regions. Thus, positive regions will appear to contain more sources than regions where positive charge is breaking down into negative charge regions. Caret et al. (2005), Ely et al. (2008) and Hodapp et al. (in press) looked at LDAR sources in MCS storms finding that the LDAR sources had an increased density both in the convective region as well as a cascading region sloping downward in the stratoform region toward the melting layer. It was also determined that different regions within a storm complex exhibited different flash characteristics such as higher peak currents in the stratoform region than in the convective core. Not discussed are the more general patterns that appear in comparisons between multiple storms in a given area and the relationship between intracloud data as provided by LDAR (or LMA) networks and the NLDN. It is emphasized that this work only examines flashes which were detected by the NLDN and that purely intracloud flashes are not part of this study.

As previously established by Orville et al. (2002), there are general relationships between multiplicity and peak current over a large sample space. Likewise, cloud to ground activity also displays relationships with respect to flash extent and mean heights of detected VHF sources.

3. ATMOSPHERIC RADIO FREQUENCY SOURCE POSITION DETERMINATION

Positioning via time-of-arrival methods is accomplished by establishing a geographically separated set of receivers and noting the time at which the radiation from a given impulse arrives at each station. If each station's precise latitude, longitude, and altitude above a reference geoid is known with a timekeeping means accurate to within a few nanoseconds, the resulting three-dimensional location of the point source may be determined via manipulation of equation 3.1. In this case, a radiation point source located at (x,y,z) is received at location (x_i,y_i,z_i) at time t_i where c is the velocity of propagation. The actual time that the source is emitted (t) is, at first glance, computed simply by iteratively solving for t using equation 3.1 for each sensor's location and timing information (Thomas et al, 2004).

$$c(t - t_i) = \sqrt{(x - x_i)^2 + (y - y_i)^2 + (z - z_i)^2} \quad (3.1)$$

Unfortunately, an iterative convergence technique is not practical for real-time applications and therefore another method is preferred which creates a linear set of equations which may be solved via matrix manipulation techniques. The method of mathematically deriving each source's position is described in Thomas et al. (2004) and Koshak et al. (1996). A graphical representation of the geometry involved is depicted in figure 3.1.

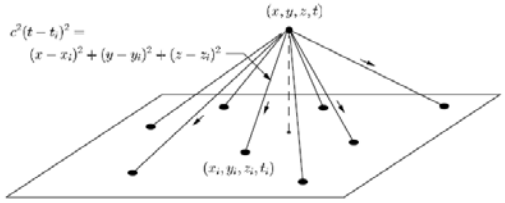

Figure 3.1 Basic TOA technique. Measurements of the arrival times t_i at N≥4 locations are used to determine the location and time of the source event(x,y,z,t) [Source: Thomas et al. 2004.]

The basic solutions provided by Koshak 1996 are intended to address positioning in a Cartesian space. The most significant errors to this method include altitude deviations caused by the Earth's curvature, which is well understood and correctable, and propagation anomalies induced by changes in the refractive index, which is also understood, yet difficult to measure. In the classic example, a nocturnal, highly stable and stratified boundary layer exists in association with a slow moving high pressure system. These conditions occur several times per year along the Gulf Coast of the United States. Warm and very moist air is present in the boundary layer capped by a strong temperature inversion and much drier air aloft. As a result, the atmosphere's index of refraction sharply changes in a short vertical space such that the velocity of propagation is altered significantly near the surface where the velocity of propagation is slower than in the drier air above. The velocity of propagation in the moist sector often slows by a factor of 0.035% as compared to the velocity of light in a vacuum whereas in the dry layer a few thousand feet above the surface may support velocities slowed by a factor of 0.025%. At 100km ranges, this can induce horizontal errors on the order of 10 meters or more. Vertical results can be grossly in error.

The illustration in figure 3.2 provides two example flashes. Source A travels primarily through the faster portion of the atmosphere whereas source B travels through the slower region. Relative to each other, even if A and B are above the same location on the earth's surface, source B will appear, to the network, farther from the network than source A due to the slower propagation time.

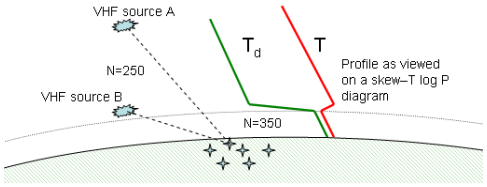

Figure 3.2 Geometry of propagation velocity anomalies due to vertical temperature and moisture gradients. Values of N represent a reduction of velocity equivalent to (N)·(10-^{6}) the speed of light.

Under mixed boundary layer conditions, the transition from lower velocities near the surface to higher velocities above is markedly more gradual increasing to 0.02% slower than the velocity of light at 600mB (Thomas et al. 2004). Still, atmospheric profiles of temperature and dewpoint are not sampled at sufficient resolution temporally or spatially to eliminate these errors.

Thomas et al. (2004) describes a tendency for distant source solutions to increase in altitude. This characteristic is observed on the Houston network as well especially at distances of 150 km or more. Boccippio et al. (2007) found that theses anomalies were largely due to radial errors such that at distances of 200 km, 4 km height errors are common.

In addition to naturally induced anomalies of propagation, an accurate and stable timing reference within the sensor must be used to accurately determine the arrival time of lightning induced RF signatures. An error of 11μs roughly corresponds to an error of 300 meters. It is the author's experience that most GPS receivers produce a one pulse per second signal accurate to ± 1 μs. This results in a source of significant error if not mitigated. While the author has experience with GPS controlled timing references accurate to within a few parts per billion for frequency control, the LDAR sensors used in Houston do not contain an ovenized oscillator capable of producing this order of accuracy. Oscillators built into self regulating oven chambers experience less thermal drift and thus can produce, when combined with an adequate reference signal, such as GPS, a highly stable and accurate time base. The actual stability and accuracy of the internal LDAR II timing circuitry is proprietary and not known.

To further mitigate errors in positioning, the network uses a method of selecting the six "best" sites for each flash based on the minimization of the Chi-square (χ^2) error. The Reduced Chi-Square (RCS) value for each VHF source located is computed via equation 3.2 from the LP5000 User's Guide.

$$RCS = \frac{\sum_{j=1}^{n}\left[\frac{m_j - m_j^*)^2}{e_j^2}\right]}{x} \quad (3.2)$$

Where:

n = Total number of measurements
j = Measurement index
m_j = Measured value
m_j^* = Calculated value based on optimum location
e_j = Theoretical measurement error (standard deviation)
x = Degrees of freedom

A study of the Lightning Mapping Array (LMA) in use during the STEPS project by Thomas et al. (2004) indicated typical RMS horizontal errors of 300 to 600 meters at distances of 100km from the network center. These findings were based on the tracks of aircraft and balloons capable of accurate geolocation fixes.

Houston LDAR performance, due to its line of site nature and relatively close spacing of the sensors performs best at ranges close in to the network. Based on general observations, including a study by Ely et al. (2008), the network detection of VHF sources is maximized within 90 km of the network center. Outside of this ring, network performance drops substantially as evidenced by comparisons of a mesoscale convective system which moved across the region on 31 October 2005. Thus, this work concentrates on events centered within approximately 60 km of the network center such that flashes extending in the region 60 km to 90 km from the center should provide good data.

Network VHF source position accuracy was also estimated in the 31 October 2005 case using geo metric model presented in Rison et al. (1999) and Thomas et al (2004). It was determined that the RMS timing error was on the order of 80 ns which corresponds to median three dimensional position error of about 250 m.

A comparison of LDAR and LMA networks was performed in Krehbiel et al (2008) for the Dallas/Fort Worth (D/FW) network. Over the past few years, it was noticed that the LMA

system tended to show a much denser cluster of VHF source points. It was speculated that a system minimum detectable signal level was approximately 15 dB better for the LMA network. For this analysis, LMA sensors were deployed alongside four existing LDAR sensors in the D/FW area. The resulting calculated noise floor of the network was about -63 dBm for the LDAR network and -78 dBm for the LMA at the Mesquite, TX site. In contrast, due to high noise levels and automatic threshold adjustments on the LMA, the LDAR sensor at the Federal Aviation Administration site was 8 dB better. Thus, the LDAR may demonstrate advantages in noisy electromagnetic environments. Insofar as positional accuracy, the two networks appear very close.

A comparison was also examined between cloud-to-ground and intracloud events between the LDAR and LMA networks. The LMA, as expected due to higher sensitivity, better detected the cloud-to-ground event in addition to also detecting corona discharge. As such some bias, with flash extent, may be possible due to sensitivity concerns.

Overall, the D/FW LDAR network exhibited good flash detection efficiency for intra-cloud and positive cloud-to-ground flashes. However, negative cloud-to-ground flashes and the intra-cloud lower charge region appear to not be handled as with the same robust nature as the LMA (Krehbiel et al., 2008).

Naturally, these biases will also appear in the Houston network as well since the D/FW LDAR system uses the same equipment. Nevertheless, this work is still considered of value with the caveat that instrument errors must be considered.

4. THE NATIONAL LIGHTNING DETECTION NETWORK

Late in the 1970s, data began to be collected on cloud to ground lightning discharges with the deployments of a number of networked lightning sensors in the Western United States and Alaska to aid in forest fire mitigation. This network was comprised of low frequency loop antennas in an orthogonal configuration plus an electric field antenna to obtain unambiguous azimuthal information with an accuracy of two degrees or better (Krider et al. 1980). Shortly thereafter, other networks were established in the United States. In the northeastern United States, a network, with an operations control center at the State University of New York at Albany, was initiated in the spring of 1982. A year later, a total of ten sensors were deployed with coverage roughly extending from North Carolina to extreme southern Quebec (Orville et al. 1983).

A mid-western network, with four sensors, was operated by the National Severe Storms laboratory in Oklahoma to complement ongoing electric field studies (Mach et al. 1986). The Oklahoma network was uniquely positioned to sample severe and tornadic thunderstorms.

By 1989, all three networks had expanded and were merged into the National Lightning Detection Network (NLDN) providing coverage for the contiguous United States. The system was upgraded in 1994 through 1995 with roughly half the sensors incorporating time-of-arrival and magnetic direction finders known as improved accuracy from combined technology (IMPACT) sensors. After the upgrade, the network included 106 sensors with an average baseline near 300 km (Cummins et al. 1998). In 2004, all sensors were upgraded to more sensitive IMPACT-ESP units and additional sensors were added to the network (Biagi et al. 2004). Today, the network covers the United States (114 sensors) and much of Canada (87 sensors) and is known as the North American Lightning Detection Network (NALDN). Figure 4.1 contains the most recently available map of NLDN locations in the contiguous United States. Vaisala, Inc. in Tucson, AZ provides ownership, operations and maintenance for the network.

Figure 4.1 Current NLDN map. System is comprised of 114 lightning sensors locations across the continental US [Source: Vaisala, 2004.]

Post-processed archive NLDN data are received monthly at Texas A&M and provide raw stroke data which includes geolocation information, stroke current (including polarity) and nanosecond-resolution timing. Using geolocation and timing information, flash multiplicity is derived. With the addition of peak current, these data provide four useful metrics to describe the characteristics of C-G lightning (Biagi et al. 2007).

5. THE HOUSTON LIGHTNING DETECTION AND RANGING NETWORK

While NLDN data provide insight into cloud-to-ground flashes, lightning also exhibits a volumetric distribution in thunderstorms that cannot be mapped by low frequency (1 kHz to 1 MHz) systems. However, VHF systems are able to obtain details about the structure of lightning flashes by measuring radio frequency burst on the order of a few microseconds (Mazur et al. 1997). By using multiple, geographically spaced, receivers, the location of the pulse origin may be found using Time of Arrival (TOA) methods assuming line of sight propagation at the speed of light through the atmosphere. While errors due to change in velocity of propagation are possible, primarily induced by the variation of vertical gradients in moisture (Freeman 1987), these errors, especially in the domain on the order of 100 km, are normally small when thunderstorms actively mix the environment.

The Department of Atmospheric Sciences at Texas A&M University has deployed a network of twelve TOA lightning detection and ranging (LDAR) sensors in the Houston area. A photograph of the Williams Airport site is included in figure 5.1. The network is centered at 29.79 N, 95.31 W. These sensors are arranged in an outward spiral with average baseline of 25 km between sensors and an average network radius of 75 km. Figure 5.2 provides an overview of the sensor locations throughout the Houston area.

Figure 5.1 LDAR sensor at the Williams Airport in far north Houston

Each sensor has a power supply, Linux based mini-computer, vertically diversified set of three antennas, GPS receiver for synchronization and radio receiver. The receiver, based on testing with RF equipment, has a nominal bandwidth of 6 MHz and employs an amplitude detector. The sensor decimates real-time data in 200μs bins (up to 10,000 transients per second). However, under quiescent conditions, the sensor is adjusted for 5% to 10% detected amplitude (500-1000) transients (from the noise floor) for optimal sensitivity. Undecimated data are stored on 80GB hard drives located at each of the twelve sites. Every few months, disk drives are collected from the sites and returned to College Station for reprocessing. The data from the disks are copied to the LDAR storage array. Storm activity days are logged for reprocessing, subsequent display and analysis.

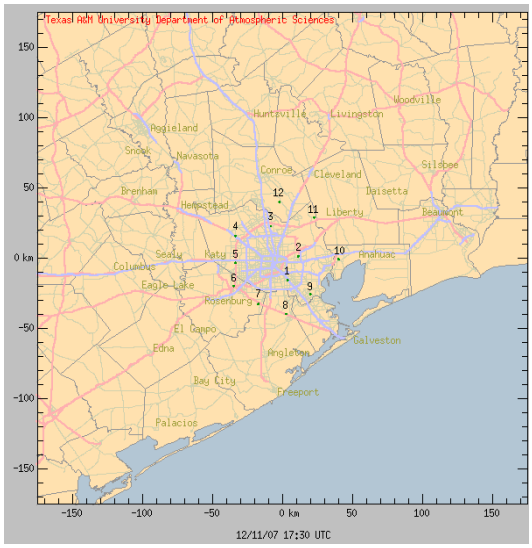

Figure 5.2 Location of LDAR sites around Houston, TX

The frequency of operation and sensor gain is remotely adjustable. The Houston network has operated on a total of three RF frequencies during its lifespan. The original deployment operated near 69 MHz, a vacant television channel in the immediate area. However, with the occurrence of troposphere propagation enhancement along the Gulf Coast, the radio frequency noise floor often increased substantially during the night due to the reception of distant television stations. E-layer "skip" propagation also contributes to an increased noise level especially during active solar conditions. Paging transmitters in the Houston area above 70 MHz also contribute to interference and regularly impact the network.

Meteor scatter proalso provides a generally small, but measurable increase in the noise floor.

To counteract the interference faced by operating within the VHF-TV band, a move was made to 113 MHz in the normally quiet aeronautical navigation band. Unfortunately, strong noise transients were observed at several locations on this band, possibly due to IF rejection issues. The source of the transients was never identified, but the decision was made to try a lower frequency band as it was not known how well the sensors would perform at higher frequencies. It should be noted that an in-depth analysis of the intermediate frequency and out of band rejection of the LDAR receivers was not performed.

In March 2007, a move to 40 MHz was made and this band has proven to be the most stable, from a noise level perspective—at least while solar activity is relatively low. Additionally, a substantive improvement in distant source detection was realized with this change. For the first time, sources as distant as the Dallas/Fort Worth area were detected.

Ensuring that the sensors are optimized from an RF perspective is one of the most time-consuming tasks with the network. Adjusting the gain of the receivers must optimally be performed each day so as to maintain adequate sensitivity without consuming excessive disk space. Various methods for automatically adjusting the gain have been discussed, but no technique has been implemented to date. If too short a time constant is selected, long duration thunderstorm events will be adversely affected by a decrease in sensitivity after gain reductions are initiated. With a longer time constant, excessive disk usage will remain an issue albeit less than via manual intervention.

The number of sensors required for VHF source solutions is configurable within the network, but is nominally set for a minimum of six. The allowable minimum and maximum altitudes for solutions are set at 0 km and 20 km respectively. Solutions falling outside these ranges are rejected as erroneous. Thus, while it may be possible to capture sources from transient luminous events, such as sprites, blue jets and elves, this network is not configured to capture any information from these phenomena.

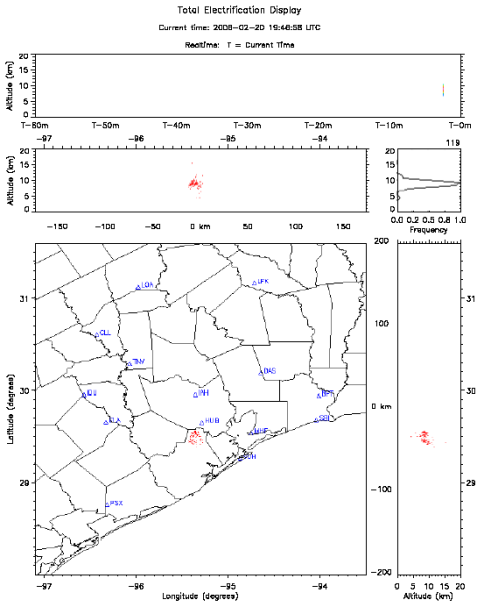

Figure 5.3 A single flash example on the TED display.

The Houston network provides a three dimensional perspective of each detected source with geolocation, timestamp, and signal strength information. A large flash may be comprised of hundreds of sources thus revealing the structure of the flash as well as flash extent.

Prior to this work, the Vaisala software, Total Electrification Display (TED), was primarily used to analyze flash data. A single flash is provided in figure 5.3 with dots indicating the derived location of lightning sources. Unfortunately, the software is not optimized for a flash-by-flash analysis of VHF source data and is cumbersome and slow to navigate across multiple flashes.

To manually correlate NLDN stroke data with LDAR data would be difficult. Therefore, new software was developed to specifically correlate LDAR data to NLDN data and display the results on a two dimensional map. The user may then graphically, based on the temporal and spatial nature of the two datasets, accept or reject the flash and its characteristics including horizontal and volumetric extent, mean altitude, multiplicity, and other metrics. While the back-end functionality is better suited for this study, the graphical display of the new software is similar to the main window of the TED display without map overlays. However, both CG and VHF sources are simultaneously displayed. CG sources are indicated by a "-" or "+" and LDAR sources are represented by dots as shown in the TED screenshot.

6. DATA AND METHODOLOGY

At the time of the study, the LDAR system operated most optimally, based on current noise/interference levels, at a frequency of 40 MHz. The study was therefore performed exclusively with 40 MHz data collected from May to July 2007. Data were collected with typically 10 to 12 sensors providing input to VHF source solutions.

When the sensor detects issues, such as poor GPS information, or a lack of synchronization pulses, it alerts the user to the anomaly such that data corruption is minimized. Nevertheless, maintenance issues sometimes appear rendering sensors fully inoperative and unavailable for data. As six sensors are required for locations, the extra sensors merely serve to increase the accuracy and detectability of individual sources.

As thunderstorms during the period March through May occur most frequently as part of mesoscale convective systems containing large expanses of intense lightning data, this period of time is not optimal for capturing single flash events. In order to help mitigate the effects of storm environment, a number of storm days were examined. The period used in this study was characterized as an extended wet period caused by a mid-level weakness between the virtually stationary Bermuda and Southwestern US high pressure areas. Several days provided useful data and while isolated storms would have been the easiest to analyze, they are not typical across Southeast Texas. Quite often, the sea-breeze initiates thunderstorm activity with storms forming nearly simultaneously along the sea-breeze axis. During the study period, synoptic forcing was quite weak as evidenced by upper level charts from that time. Most of the storms in the analysis were of the multi-cell variety and thus yielded high percentages of unusable flashes primarily due to sympathetic lightning, as described in Mazur (1982). Additionally, other nearby storms could independently generate an unrelated flash. It is recognized that this induces a potential bias in the results, but without the ability to separate such events in a timely manner; contaminated flashes will not be considered. That is certainly not to say that they are not significant, but rather hard to measure.

Each month Vaisala archives NLDN data that have been post-processed and are of a higher accuracy than the real-time NLDN feed. LDAR data are also collected in real time in a decimated (lossy) format. However, every few months, the disk drives, located within the sensor, are collected and all flash data are reprocessed using the complete non-decimated data. Any data gaps are filled using decimated data.

It should be noted that Vaisala has filtered all positive flashes with median peak currents of less than 15 kA after March of 2006. This was verified by examination of the dataset on-hand at Texas A&M University. These were determined to largely be comprised of intracloud-only flashes. This limit consideration started based on initial work by Wacker et al. (1999a and 1999b) and Cummins et al. (1998) recommending a 10 kA lower threshold for discriminating between intra-cloud and cloud to ground flashes. The threshold was later modified to 15 kA after subsequent findings of Biagi (2007) whereby it appears that NLDN positive strokes of less than 10 kA appear to be mostly intracloud discharges and those above 20 kA tend to be mostly cloud-to-ground discharges. The 10 kA to 20 kA region appears to be a transition zone where ambiguity exists. Therefore, as a compromise, yet indefinite solution, 15 kA became the lower limit of positive strokes in the NLDN dataset. No data exclusions are apparent for negative flashes.

A box, defined as the region with upper left coordinate of (30.3N, 95.77W) and lower right coordinate of (29.3N, 94.77W), hereafter known as the NLDN domain, was defined to geographically select NLDN derived cloud-to-ground flashes for analysis. This area constitutes the peak performance region for the Houston LDAR network. Since spatially large flashes of over 75km in length have been observed in the network (Ely et al, 2008 and Hodapp et al., 2008), a much larger area was chosen to search for LDAR sources corresponding to the location and time of the cloud-to-ground flash. This larger area, bounded by an upper left coordinate of (31.8N, 97.27W) and lower right coordinate of (27.8N, 93.27W) served as the LDAR domain. The geographic extent of both domains is presented in figure 6.1.

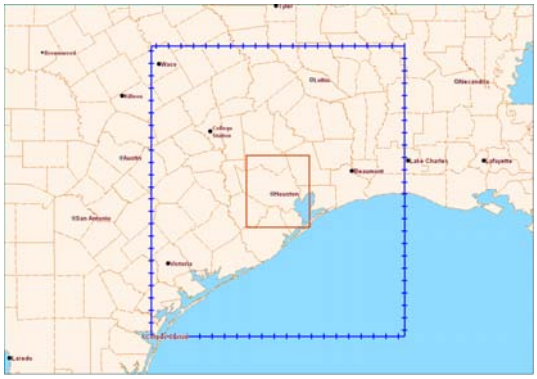

Figure 6.1 NLDN and LDAR domains. NLDN flashes which occurred in the red box were selected for analysis for comparison to LDAR sources detected within the blue box.

Unfortunately, the complexity surrounding temporal and spatial patterns of lightning results in characteristics that are not trivially solved with computer algorithms. While some automation may be possible, such an exercise exceeds the scope of this work. Therefore, manual analysis of each flash was performed to ensure an accurate representation of total lightning characteristics.

Using the software, written by the author, NLDN data corresponding to a known thunderstorm period are extracted for analysis. All strokes that fall within the NLDN domain during the elected time period are stored in a file. For a given storm day with activity within the NLDN domain, the cloud-to-ground flashes were analyzed sequentially, in time. For each NLDN detected CG found within the domain, a corresponding search of LDAR data was made within two seconds of the first CG stroke. The user is then provided a graphical plan-view representation of all NLDN strokes and LDAR sources found during that time. Source by source text data are also available at decision time to ensure that no obvious temporal gaps exist in the discharge pattern. NLDN negative strokes are represented by a white "+" and positive strokes are shown as a red "+". LDAR sources, being much more numerous, are depicted as yellow dots. The user is then able to accept or reject each flash based on the data presented checking for continuity both spatially and temporally. All accepted flashes appeared to be comprised of one lightning flash. The rate of acceptable to unacceptable flashes, for those examined in the study, is estimated to be 1 in 5 to 1 in 10.

In this analysis, the following criteria were used in accepting flashes. Every NLDN stroke must be located within 10 km of subsequent strokes and have inter-stroke timing of less than 0.5 seconds as used in Orville et al. (2002). It is desired that NLDN flashes must not be contaminated with sympathetic flashes (described in Mazur, 1982) in attempt to focus on single events. This may introduce a bias, but in light of the issues surrounding much greater reported flash extents when nearby storms flash simultaneously, it is believed that the elimination of contaminated flashes is justified. Prior NLDN detected flashes must be separated by at least 2 seconds from the flash under analysis. LDAR sources must appear to qualitatively appear to be the result of a single flash with no significant (more than a kilometer or two) breaks in branching. LDAR sources are examined for two seconds either side of the NLDN determined flash event. Thus, we establish a qualitative spatial and quantitative temporal restriction on events.

A two second flash analysis time was selected as certain flashes (especially "anvil crawlers") tend to have long life spans and the intent is to not artificially reduce the flash extent by limiting the maximum time of the flash. While comprehensive data regarding the duration of VHF source events were not available, two seconds either side of the NLDN event was chosen as a reasonable compromise based on previous visual lightning observations, the high flash rates observed, as well as the findings of Carey et al., (2005) who found flash durations of just over three seconds. Thus, the four second window chosen here is believed adequate to cover most cases. Height information was extracted from LDAR data and the average height of all detected VHF sources, for each flash, was obtained.

If no LDAR sources were found to correlate with the NLDN flash, the flash was marked as a "miss" for detection efficiency calculations. In this case, correlate means that a LDAR flash event was not observed with a corresponding NLDN flash event within 10 km of the LDAR flash extent or within two seconds before or after the NLDN flash. In this case, two possibilities exist: Cloud-to-ground flashes occurred without creating any VHF sources or, more likely, cloud-to-ground flashes occurred that were too weak to detect with the LDAR network.

To obtain a metric for flash extent, a geographic 200 by 200 bin horizontal grid system was developed over the LDAR domain. This grid results in a North / South height of 2.22 km and East / West width of 1.93 km at grid center resulting in an area of roughly 2.1 km^2. In the

vertical, the atmosphere was cut into layers of 1 km from 0 to 20 km. These grids are hereafter referred to horizontal bins and volumetric bins. When a VHF source was detected in a bin that bin was marked as active and the analysis of additional sources continued. When the LDAR entire flash period was parsed, the resulting active bins indicate the horizontal and volumetric extent for that flash. The software automatically calculates the horizontal and volumetric extent as well as the mean altitude for each manually accepted flash.

The analysis of flashes with multiplicities greater than ten is hampered by the low occurrence of such flashes. To make some use of the acquired data, flashes exhibiting multiplicity greater than 10 were aggregated into a category named "10+."

In southeast Texas, the ratio of positive to negative flashes typically runs near 10% annually with higher positive rates during the winter (Orville et al. 2002). Statistics were collected on positive and bipolar (positive first, then negative and negative first, then positive) flashes and then compared with the more common negative-only flashes.

In order to verify multiplicity and peak current, after the flashes were manually selected, Microsoft Excel was used to validate cloud-to-ground stroke multiplicity and peak flash current. Correlation of LDAR flash extent with individual cloud-to-ground strokes is, at best, a difficult undertaking especially when well over one thousand flashes have been selected. Therefore, peak current was chosen to represent the amount of discharge in each flash. After the post-processing exercise with Excel, the values of location, time, peak current, multiplicity, horizontal and volumetric extent, and mean VHF source altitude are available.

Analysis of the data was performed with tools in Microsoft Excel using macros for median, mean, standard deviation and trending.

A sanity check on the dataset was performed, using average multiplicity, peak currents, and percent positive flashes, comparing the findings of Steiger et al. (2002). Values were found to be within reasonable range of the annualized averages obtained previously for southeast Texas taking into consideration the time period of this study.

It should be mentioned however, that the LDAR system tends to prefer detection of events into positive charge regions (Wiens et al., 2005). These regions tended to exist near 5 km and 10 km in most storms in this study as well as other storms observed along the Texas Gulf Coast. A comparison of interferometric systems, which tend to detect fast negative break downs (characteristic of stepped-leaders) versus the slow breakdowns that are well detected, with LDAR demonstrates that the LDAR sources detected are higher than those detected by the interferometer. Neither system detects all of the activity in a given flash (Mazur et al., 1997). Therefore, some positive height bias in the LDAR results is possible.

7. RESULTS

A total of 1407 flashes were analyzed as part of this study with comparisons of each of the five variables under investigation: multiplicity, peak current, horizontal flash extent, volumetric flash extent, and mean altitude.

576 single-stroke flashes were collected along with a total of 831 multi-stroke flashes with a mean multiplicity of 3.3 and standard deviation of 3.1. A pseudo-exponential decay in events vs. multiplicity is evident in the graph in figure 7.1. 56 Flashes contained at least one positive stroke and 29 flashes were single stroke positive events. All flashes with multiplicity of 10 or greater were aggregated into a single category: "10+".

Comparing the non-weighted median height of all negative flash VHF sources detected by the LDAR network with multiplicity reveals that single-stroke flashes exhibit significantly greater vertical extent than those with two or more strokes. The results of these data are shown in figure 7.2a. While deviation was generally limited to +/- 500m on flashes with multiplicity greater than two, single stroke flashes averaged almost 2 km higher. Mean heights closely follow the trends revealed with median heights, but have slightly less variation among multiplicities. The variability of VHF source heights decreases with increasing multiplicity with standard deviation values of single stroke flashes near 3 km generally decreasing to near 2 km with ten or greater strokes per flash. VHF source heights were not binned, but rather depict the detected heights of all flashes as indicated by the LDAR network for each corresponding value of multiplicity. Positive and bipolar flashes had a similar trend with multiplicities greater than three. However, the lack of a significant number of sample flashes precludes inclusion in the analysis.

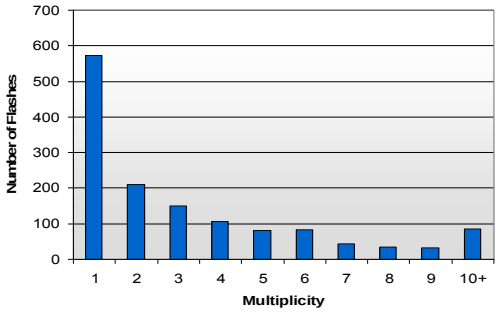

Figure 7.1 Histogram of multiplicity for all flashes analyzed in this study. Flashes with multiplicities greater than 9 are grouped into the 10+ category. Of the flashes shown here, 56 contained at least one positive stroke.

At the 2008 AMS Conference in New Orleans, Dr. Kyle Wien suggested looking at median height in addition to mean height. From that recommendation, it was seen that the single stroke deviation was somewhat greater as compared to greater multiplicities. In effect, it shows a slightly more pronounced signal in this case. However, the mean and median heights are highly correlated and are assumed to be interchangeable. The median is not always higher or lower than the mean and the deviations appear to be the result of statistical noise. As the goal of this work is to demonstrate trends with many flashes, mean values are used for the remainder of the work.

Figures 7.2a and 7.2b compare the same two metrics, but figure 7.2b display all available mean height information from all negative flashes, Not only do single stroke flashes have a greater mean and median height, but they also have the greatest overall height in the sample set. As every flash under consideration in this study had a ground contact point, it is believed that an examination of lowest heights is not legitimate as all flashes are assumed to have ground contact. As Krehbiel et al (1984) found, low altitude sources are not detected as readily because the LDAR system has a tendency to locate sources close to the positive end of the discharge. As positive flashes, especially between 15 kA and 20 kA may be falsely indicating ground contact, there is the potential for bias. However, the analysis of multiplicity and peak currents with height included herein is made with negative-only flashes outside of tables 7.1-7.3.

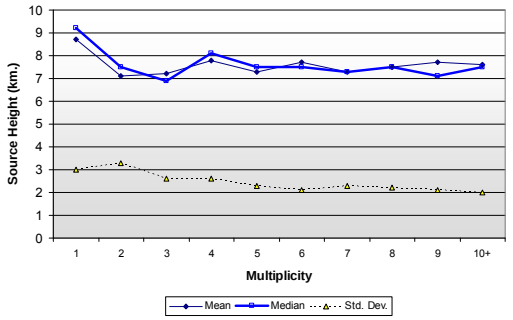

Figure 7.2a Negative flash multiplicity versus the median, mean, and standard deviation of all VHF sources detected by LDAR. Notice the substantial deviation for single-stroke flashes with multiplicities 2-10+ being fairly flat.

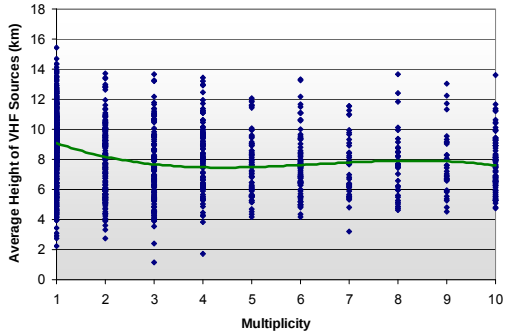

Figure 7.2b Scatter plot of negative flash mean height VHF sources vs. multiplicity. The solid green line indicates a sixth-order polynomial chosen to give a feel for the general trend for the data. Note the relative flatness of multiplicities 2-10+ and the increase associated with single stroke flashes.

One of the most anticipated metric comparisons for this study was the relationship between multiplicity and flash extent and this exercise yielded results in line with expectations. The network was divided into 2 km by 2 km bins horizontally with 2 km by 2 km by 1km volume bins. The results are shown in figure 7.3 and are the basis for flash extent comparisons. Only negative flashes were used in this figure. Inclusion of positive flashes did not significantly change the results.

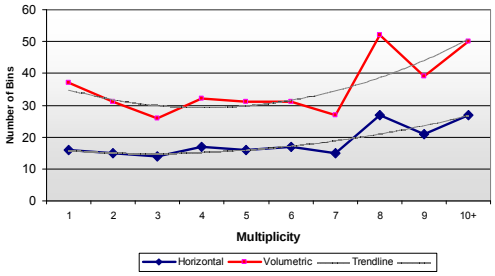

Figure 7.3 Negative flash multiplicity vs. flash extent. The red line indicates volumetric bins. The blue line indicates horizontal bins. Two second-order polynomial trend lines are provided corresponding to each curve above.

As expected, variance among individual flashes was high. A trend toward increasing flash extent, both horizontally and volumetrically is shown via trend lines. Both horizontal and volumetric trends data track very similarly with only a nearly constant factor between the two. That is, the number of volumetric bins is roughly twice that of number of horizontal bins.

Based on these data, it appears plausible that single stroke flashes are more vertically oriented. General observations of negative flash observations of 2006 and 2007 warm season thunderstorms reveal a marked peak in the occurrence of VHF sources near 10 km. A significantly lower amplitude secondary peak near 5 km, in a multiple charge layer configuration, is also evident as described in Marshall and Rust (1991). It is therefore theorized that flashes of higher multiplicities tend to propagate more readily within the anvil positive charge region drawing from a larger region from which to support multiple strokes. As the relationship of 2-D to 3-D bins is not cubic, but rather a factor of two, the flash spreads more horizontally than vertically. The tortuous extent of the flash, based on these data, spreads most readily in the anvil region within a narrow vertical corridor.

Figures 7.4 and 7.5 illustrate the data gathered comparing flash extent with the absolute value of peak current. The scatter plots presented in these two figures have significant flash-to-flash variance. Unfortunately, no detectable signal was observed and as such, there appears to be no correlation between peak current and flash extent.

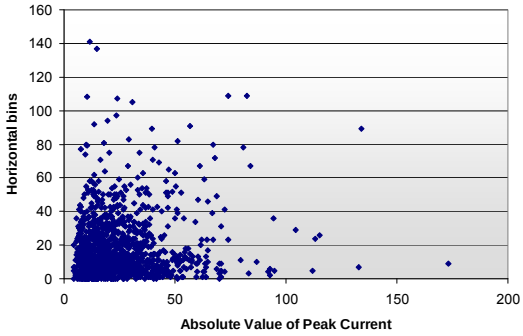

Figure 7.4 Scatter plot of the number of horizontal bins for negative flash VHF sources vs. peak current.

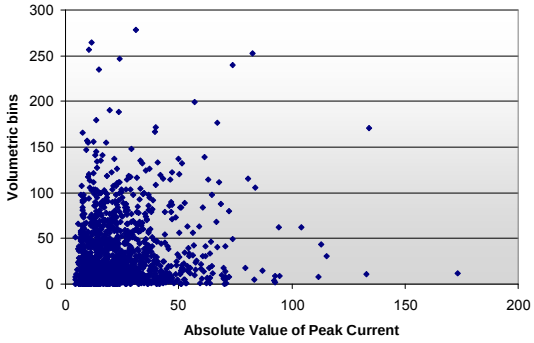

Figure 7.5 Scatter plot of the number of volumetric bins for negative flash VHF sources vs. peak current. The green line indicates a second-order polynomial trend line.

The flash data gathered in this study were 96% negative with the large majority of positive flashes being single stroke. The NLDN detected positive flashes yielded a different signature where current peaked with a flash multiplicity of two. Orville et al. (2002) found that increasing multiplicity yields increasing peak currents for negative flashes via NLDN. The trend of 1998-2000 data shows a linear relationship with multiplicity and flash extent and is presented in figure 7.6. Multiplicity and flash extent appear to be directly related. It is plausible that, for aggregated measurements of Southeast Texas flashes, some assumptions may be valid inferring an average flash extent especially given peak flash current. The relationship, while not as linear, appears also to hold between multiplicity and flash extent. This is not to say that flashes of high multiplicity always yield large flash

extents. However, given the number of sample flashes, a relationship appears to exist.

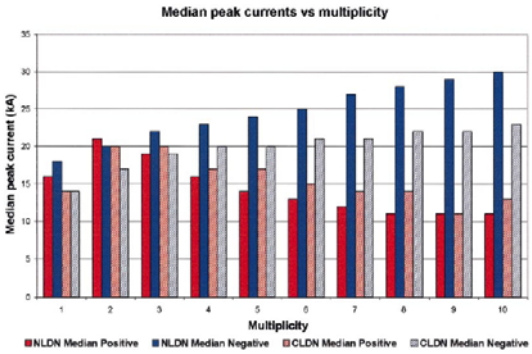

Figure 7.6 Median peak current plotted as a function of the flash multiplicity for each polarity. Information provided for both networks-- the NLDN and the CLDN [Source: Orville et al. 2002.]

The average height of VHF sources trends downward with increasing peak current, at least with peak current values of less than 100 kA. There is low confidence in the noted trend with flashes of peak current greater than 100 kA, shown in figure 7.7, as only eight flashes exceeded this threshold. The lower threshold for peak current for the flashes examined was -4 kA, which had average VHF source heights above 10 km. The trend analysis quickly brings the mean height down to near 8 km with -15 kA flashes. This 8 km level holds through about -60 kA before beginning a downward trend. As mentioned before, it is theorized that flashes with increasing current spread horizontally in the anvil region and the trend noted here could plausibly support that assumption. Previously, ambiguity was discussed for low-current positive flashes. Only negative flashes were considered with the height vs. peak current analysis. There are no known issues with incorrect NLDN detection of negative flashes as intra-cloud lightning.

It appears that the height maximum seen with multiplicity and peak current match trends implied by flash extent analysis as supported by the horizontal and volumetric bin data and theory that with increasing multiplicity and extent flashes tend to spread more evenly in the anvil region. Once again, low multiplicies or peak currents point to higher, perhaps more vertical flash events.

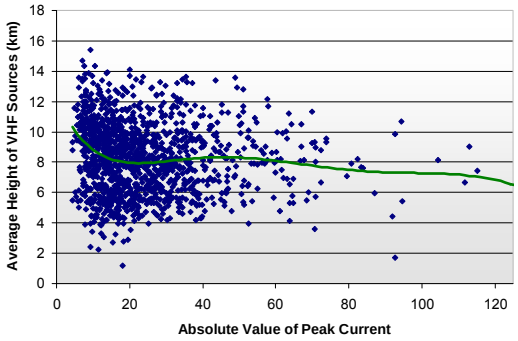

Figure 7.7 Scatter plot of mean height of negative flash VHF sources vs. peak current. The solid green line indicates a sixth-order polynomial trend. Only eight flashes occurred with peak current greater than 100 kA and thus flashes exceeding 125 kA are removed.

During the sample storms, a total of 57 flashes contained at least one positive stroke within the flash. Of these, 29 flashes were single stroke, 3 were multi-stroke positive, 12 had at least one negative stroke followed by at least one positive stroke, and 13 had one positive stroke followed by at least one negative stroke. Flashes that contain both positive and negative strokes are called bipolar flashes. It is believed that the bipolar flashes detected with the NLDN are of type iii as defined in Rakov and Uman (2003) with return strokes of opposite polarity. All documented flashes of this type are upward propagating. A cursory check of bipolar flash positions was reviewed with the locations of known obstacles in the Federal Aviation Administration digital obstacle database. A number of bipolar flashes occurred within 0.4 km a known tower. Note that towers under 61 meters are not included in this database. The argument can certainly be made that additional positive flashes are required to gain confidence in trends. Nevertheless, the data are included here for completeness. Positive flash data came almost uniformly for all study days and both the median and mean data were virtually identical.

If all flashes are examined, flashes with positive strokes have a 0.4 km greater mean altitude. This could be related to the positive flash / intracloud flash ambiguity with the NLDN. However, negative flashes also exhibit higher mean heights with lower multiplicities and no known ambiguities exist for negative flashes. Given the findings in this work, since positive flashes tend to have low multiplicities, one would expect mean positive heights to be greater than

negative flashes in general. With a low number of flashes, the intra-flash variance is also higher with positive flashes.

If all bipolar flashes are eliminated, a significant jump in mean height is observed. The 32 positive only flashes averaged 1.1 km higher than all negative flashes. With the high percentage of single stroke events, the primary cause for this jump is believed to be low multiplicity and not factors that are specific to the microphysics of positive strokes. That is not to say that differences exist, but rather, that the trends at this level of analysis point toward multiplicity.

Of all bipolar flashes, positive first flashes had lower mean heights than negative first flashes by about 0.5 km. Positive first bipolar flashes had a lower mean multiplicity of 3.8 versus negative first bipolar flashes with mean multiplicity of 4.6. This trend is opposite that seen with other data. Clearly some other mechanism may be at work with bipolar flashes and analysis of these types of data is certainly an area for future study.

Isolating single-stroke flashes, with the exception of greater mean heights for positive flashes, flash extents, both horizontal and volumetric are quite comparable. These data are presented in table 7.1. On average, positive flashes are 0.7 km higher with a slightly greater standard deviation at 2.7. Bipolar flashes with the positive stroke first have a lower mean height.

Table 7.1 Mean height summary for negative, positive, and bipolar flashes.

All Flashes	Avg Hgt (km.)	StdDev (km.)
Negative average height	8.3	2.3
All positive average height	8.7	2.7
Positive only average height	9.4	2.8
Bipolar average height	7.7	2.2
Positive first bipolar avg height	7.2	2.2
Negative first bipolar avg height	8.2	2.1

Table 7.2 Single stroke summary for negative and positive, single stroke flash characteristics.

Single stroke flashes	Avg Hgt (km.)	StdDev (km.)
Negative average height	9.1	2.2
Positive average height	9.8	2.7
	Horz Bins	**StdDev**
Negative horizontal extent	17	18
Positive horizontal extent	18	17
	Vol Bins	**StdDev**
Negative volumetric extent	35	38
Positive volumetric extent	35	31

Table 7.3 Summary of flash extents based on type of flash both based on horizontal and volumetric extent.

Flash Extents	Horz Bins	StdDev
Horizontal Flash Extent		
Negative	18	18
Positive	17	16
Negative first bipolar	24	22
Positive first bipolar	15	11
Volumetric Flash Extent	**Vol Bins**	**StdDev**
Negative	35	37
Positive	31	29
Negative first bipolar	49	42
Positive first bipolar	31	24

Examining single stroke flashes, both with mean height and flash extent as shown in table 7.2, positive flashes tend to have greater heights. This is likely due to the low multiplicity nature of positive flashes. However, from a flash extent perspective, there is virtually no difference between negative and positive flashes on the whole.

Making a comparison between the flash extents between all flash types examined yields very similar results with one exception. As seen in table 7.3, negative first bipolar flashes tend to near 50% greater flash extent than other types. Presumably, these flashes make a different use of the overall charge structure of the storm. As noted in Hamlin et. al, (2003), the charge structure of individual flashes should be obtainable based on the breakdown pattern. This method may allow a means for some explanation of this phenomenon but is outside the scope of this work.

Finally, VHF source detection efficiency was evaluated by assuming that the NLDN detected flashes are ground truth for the occurrence of cloud-to-ground lightning. NLDN flashes which temporally and spatially correlated to LDAR sources were considered a hit. NLDN flashes,

which had no corresponding LDAR sources, were misses. Two ranges of efficiency were evaluated. The first range was a circle from 0 to 30 km from the network center. The second range extended from 30 to 60 km from the network center. The Houston LDAR network exhibited a detection of 99.6% within 30 km and 96.8% in the outer ring compared to the NLDN dataset.

While hundreds of intracloud flashes were detected by the LDAR network that were not detected by the NLDN (as expected), intracloud evaluations were outside the scope of this study. Nevertheless, the two networks are complementary. By noting the time of ground flash, corresponding VHF sources can be analyzed keeping in mind that low current, positive flashes may be incorrectly reported as a cloud-to-ground event.

Thunderstorm characteristics also change somewhat depending on the maturity of the storm. Qualitatively, in the early period of a storm's lifetime, flash extents tend to be lower in altitude and exhibit limited flash extents. This is due to the spatially limited nature of the still non-mature storm. As the storm matures and the anvil becomes established and spreads, average height and flash extents increase with the addition of small, positively charged ice especially at anvil levels.

8. CONCLUSIONS

An examination was conducted of lightning flashes for warm-season Southeast Texas thunderstorms from May to July 2007. The data collected by this analysis identify several key findings of total lightning characteristics based on the 1400 flashes analyzed. While inter-flash variance is quite high, trends are evident in the data.

Single stroke flashes are unique in that they have greater median and mean flash heights than their multi-stroke counterparts. While some variations exist with multi-stroke flashes, these multi-stroke events were centered near 7.5 km while single stroke events were centered near 9 km. The standard deviation among flash events tended to decrease (become less variant) with higher order multiplicities.

Flash extent trends upward with increasing multiplicity. Horizontal and volumetric trends were offset by a nearly constant delta for all multiplicities. This implies that with increasing multiplicity, flashes tent to increase more horizontally than volumetrically. Flashes with ten or greater strokes are 50% more expansive volumetrically than single stroke flashes and 2.1 times more expansive horizontally than single stroke flashes.

Flash extent, both volumetrically and horizontally appears to be unrelated to absolute peak current.

It has been shown by Orville et al. (2002) that negative flash currents increase monotonically with multiplicity. This work was comprised of 96% negative flashes. There appears to be a direct relationship also with peak current, multiplicity and flash extent.

Mean VHF source height was shown to be higher for low peak current flashes (especially under -10 kA) than greater values of peak current which trend near 8 km with -10 kA to -50 kA flashes. Data, in flashes with peak currents of -75 kA or greater, were fairly sparse and while a downward trend is observed in figure 7.7, a lack of sample data leads to a low confidence in this trend. Due to the scant number of positive events and highly variant data, results are not shown here.

Comparing positive, bipolar, and negative flashes yields similar results suggesting that subtle differences exist in the flash extent or heights of such events. The outlier appears to be the greater average height of positive-only (multi-stroke) flashes as well as much greater flash extents with negative-first bipolar flashes. The positive only deviation is likely due to the enhanced vertical structure of single-stroke flashes as most positive flashes in this study were of this type. The deviation in flash extent of negative only flashes may be due to the charge structure of the storm and the means in which these types of events are triggered. Additional flashes would be required to verify this trend statistically and provide enough data to establish a theory.

Detection efficiencies, while seemingly quite high, using NLDN as a baseline, are less than what is possible with an LDAR network in a less noisy environment. Great care was taken with site selection to mitigate radio-frequency noise problems. However, Houston subjects an elevated radio noise floor to the network. Contributing to this noisy environment are electrical distribution systems, impacts from two-way and paging systems, close proximity of mass media broadcast transmitters at some sites, automobile ignition systems nearby and many others. Additionally sporadic distant sources of radio frequency contamination may occur due to ionospheric enhancements. The Houston LDAR network exhibited an average detection efficiency of 99.7% within 60 km of the network center.

With a quieter environment, the detection efficiency would improve with the added benefit

that many more sources per flash could be resolved. Software techniques, internal to the LDAR system, may also have room for improvement. Somewhat larger horizontal and volumetric flash extents are possible with increased network sensitivity, but changes in the trends found herein are not expected.

Overall, the findings of this study match well with theoretical expectations with the exception of the elevated heights and flash extent of single-stroke events as well as the relationship between peak current and flash extent. Since single-stroke flashes are very common, accounting for over forty percent of the dataset examined here, it is difficult to theorize that special microphysical process exists for just these events. Nevertheless, single-flash events and intra-cloud discharges are two areas of worthwhile study enabled by LDAR networks.

Certainly, there remain many unanswered questions in the study of total lightning. Questions such as why single-stroke flashes tend to be more vertical and what causes the apparent greater flash extent with negative first bipolar flashes remain unresolved, but certainly worthwhile to consider for future work.

REFERENCES

Biagi, C. J., K. L. Cummins, K. E. Kehoe, E. P. Krider, 2007: National Lightning Detection Network (NLDN) performance in southern Arizona, Texas, and Oklahoma in 2003-2004. *J. Geophys. Res.*, **112**, D05208, doi:10.1029/2006JD07341.

Boccippio, D. J., S. Heckman, and S. J. Goodman, 2001: A diagnostic analysis of the Kennedy Space Center LDAR network: 1. Data characteristics. *J. Geophys. Res.,* **106**, 4769–4786.

Carey, L. D., M. J. Murphy, T. L. McCormick, and N. W. S. Demetriades, 2005: Lightning location relative to storm structure in a leading-line, trailing-stratiform mesoscale convective system, *J. Geophys. Res*., **110**, D03105, doi:10.1029/2003JD004371.

Cummins, K. L., M. J. Murphy, E. A. Bardo, W. L. Hiscox, R. B. Pyle, and A. E. Pifer, 1998: A combined TOA/MDF technology upgrade of the U.S. National Lightning Detection Network. *J. Geophys. Res*., **103**, 9035-9044.

Cummins, K. L., J. A. Cramer, C. J. Biagi, E. P. Krider, J. Jerauld, M. A. Uman, V. A. Rakov, 2006: The U.S. National Lightning Detection Network: Post-Upgrade Status. Atlanta, GA, *Proceedings of the 2006 AMS Conference*, 6.1.

Ely, B. L., R. E. Orville, L. D. Carey, and C. L. Hodapp, 2008: Evolution of the total lightning structure in a leading-line,trailing-stratiform mesoscale convective system over Houston, Texas. *J. Geophys. Res*., **113**, D08114, doi:10.1029/2007JD008445.

Freeman, R. L., 1987: *Radio System Design for Telecommunications (1-100 GHz)* John Wiley, 887 pp.

Goodman, S. J., T. Blakeslee, H. Christian, W. Koshak, J. Bailey, J. Hall, E. McCaul, D. Buechler, C. Darden, J. Burks, T. Bradshaw, P. Gatlin, 2005: The North Alabama Lightning Mapping Array: Recent severe storm observations and future prospects. *J. Atmo. Res.*, **76**, 423-437.

Hamlin, T., P. R. Krehbiel, R. J. Thomas, W. Rison, J. Harlin, and Y. Zhang, 2003: Electrical Structure and Storm Severity Inferred by 3-D Lightning Mapping Observations During STEPS. Versailles, Fr., *Proc. Intn'l Conf. of Atmos. Electricity 2003*.

Hodapp, C.L., L.D. Carey and R. E. Orville, (in press):, Evolution of radar reflectivity and total lightning characteristics of the 21 April 2006 mesoscale convective system over Texas. *J.Atmos. Res.*. doi:10.1016/j.atmosres.2008.01.007.

Krehbiel, P. R., 1981: An analysis of the electric field change produced by lightning, *Ph.D. dissertation*, Univ. of Manchester Inst. of Sci. and Technol., U. K.

Krehbiel, P. R., M. Brook, S. Khanna-Gupta, C. L. Lennon, R. Lhermitte, 1984: Some results concerning VHF lightning radiation from real-time LDAR system at KSC, Florida. Albany, NY, *Proc. 7th Intn'l. Conf. Atmos. Elec*., 388-393.

Krehbiel, P. R., W. Rison, H. Edens, N. O'Connor, G. Aulich, R. Thomas, S. Kieft, S. Goodman, R. Blakeslee, J. Hall, J. Bailey, 2006: The Washington DC Metro Area Lightning Mapping Array. San Francisco, CA, *American Geophys. Union*, Fall Meeting 2006.

Krehbiel, P.R ., W. Rison, R. Thomas, and N. O'Connor, 2008: Comparison of LMA and LDAR-II Observations in the Dallas-Ft. Worth

LDAR-II Network. Tucson, AZ, *2008 Intn'l Lightning Detection Conf.*

Krider E., R. Noggle, A. Pifer, D. Vance, 1980: Lightning Direction-Finding Systems for Forest Fire Detection. *Bull. Amer. Meteor. Soc.,* **61**, pp. 980–986.

Koshak, W. J. and R. J. Solakiewicz, 1996: On the retrieval of lightning radio sources from the time-of-arrival data, *J. Geophys. Res*., **101**, 26631– 26639.

Lang, T., L. J. Miller, M. Weisman, S. A. Rutledge, L. J. Barker III, V. N. Bringi, V. Chandrasekar, A. Detwiler, N. Doesken, J. Helsdon, C. Knight, P. Krehbiel, W. A. Lyons, D. MacGorman, E. Rasmussen, W. Rison, W. D. Rust, and R. J. Thomas, 2004: The Severe Thunderstorm Electrification and Precipitation Study (STEPS). *Bull. Amer. Meteor. Soc.,* **85,** 1107–1125.

MacGorman, D. R. and W. D. Rust, 1998: *The Electrical Nature of Storms*. Oxford University Press, New York, 422 pp.

Mach, D. M., D. R. MacGorman, W. D. Rust, and R. T. Arnold, 1986: Site Errors and Detection Efficiency in a Magnetic Direction-Finder Network for Locating Lightning Strikes to Ground. *J. Atmos. Oceanic Technol.*, **3**, 67–74.

Maier, L., C. Lennon, T. Britt, and S. Schaefer, 1995: LDAR system performance and analysis. Boston, MA, *6th Conf. on Aviation Wea. Sys*., Am. Meteorol. Soc.

Marshall, T.C. and W. D. Rust, 1991: Electric field soundings through thunderstorms. *J. Geophys. Res*, **96**, 22301.

Mazur, V., 1982: Associated lightning discharges. *Geophys. Res. Lett.*, **9**, 1227-1230.

Mazur, V., E. Williams, R. Boldi, L. Maier, and D. E. Proctor, 1997: Initial comparison of lightning mapping with operational time-of-arrival and interferometric systems. *J. Geophys. Res.*, **102**, 11071– 11085.

Orville, R. E., G. R. Huffines, W. R. Burrows, R. L. Holle, and K. L. Cummins, 2002: The North American Lightning Detection Network (NALDN) - First Results: 1998-2000. *Mon. Wea. Rev*., **130**, 2098-2109.

Orville R. E., R. W. Henderson, L. F. Bosart, 1983: An East Coast lightning detection network. *Bull Amer. Meteor. Soc.,* **64**, 1029–1037.

Orville, R. E, 2008: Development of the National Lightning Detection Network. *Bull. Amer. Meteor. Soc*., **89**, 180-190.

Proctor, D. E., 1971: A hyperbolic system for obtaining VHF radio pictures of lightning*. J. Geophys. Res*., **76**, 1478– 1489.

Proctor, D. E., 1981: VHF radio pictures of cloud flashes. *J. Geophys. Res.*, **86**, 4041– 4071.

Rakov V, and M. Uman, 2003: *Lightning Physics and Effects*, Cambridge University Press, 687 pp.

Rison, W., R. J. Thomas, P. R. Krehbiel, T. Hamlin, and J. Harlin, 1999: A GPS-based three-dimensional lightning mapping system: Initial observations in central New Mexico. *Geophys. Res. Lett.,* **26,** 3573–3576.

Samaras, T. M. and W. A. Lyons, 2008: Visualization of naturally produced lightning strikes using high speed imaging (2008). New Orleans, LA, *3rd Conf. on Meteor. Applications of Lightning Data*, Amer. Meteor. Soc.

Steiger, S. M., R. E. Orville and G. Huffines, 2002: Cloud-to-ground lightning characteristics over Houston, Texas: 1989-2000. *J. Geophys. Res*, **107**, D11,10.1029/2001JF001142.

Stolzenburg, M.,W. D. Rust, and T. C. Marshall, 1998a: Electrical structure in thunderstorm convective regions Part II: Isolated storms. *J. Geophys. Res.,* **103,** 14079–14096.

Thomas, R. J., P. R. Krehbiel, W. Rison, S. J. Hunyady, W. P. Winn, T. Hamlin, and J. Harlin, 2004: Accuracy of the lightning mapping array. *J. Geophys. Res.*, **109**, doi: 10.1029/2004JD004549.

Vaisala, O., 2003: *LP 5000 User's Guide*, p. 212.

Vaisala, O. 2004: Report on the 2002-2003 U.S. NLDN System Wide Upgrade, http://www.vaisala.com/weather/products/lightning/knowledgecenter/aboutnldn/vn_2002-2003_nldn_upgrade_article_rev1_nov2004.pdf.pdf.

Wacker, R. S. and R. E. Orville, 1999a: Changes in measured lightning flash count and return stroke peak current after the 1994 U. S. National

Lightning Detection Network upgrade; Part I: Observations. *J. Geophys. Res*., **104**, 2151-2157.

Wacker, R. S. and R. E. Orville ,1999b: Changes in measured lightning flash count and return stroke peak current after the 1994 U. S. National Lightning Detection Network upgrade; Part II: Theory. *J. Geophys. Res.*, **104**, 2159-2162.

Wiens, K. C., S. A. Rutledge, and S. A. Tessendorf, 2005: The 29 June 2000 Supercell Observed during STEPS. Part II: Lightning and Charge Structure. *J. Atmos Sci*., **62**.

ACKNOWLEDGEMENTS

We gratefully acknowledge that the scientific research and operation of the Houston LDAR network are supported by the National Science Foundation (ATM-0442011 and ATM-0321052). We acknowledge Vaisala for providing the NLDN data used in this study. In addition we would like to thank the generosity of the airports, school districts, and colleges around Houston who have donated land use, electricity, and Internet connections to enable real-time operation of the network.